https://doi.org/10.31436/iiumej.v24i2.2717

PARAMETRIC OPTIMIZATION OF OIL PALM MESOCARP FIBER VALORIZATION WITH HYBRID OZONATION-ULTRASONIC PRETREATMENT METHOD

DIDI DWI ANGGORO, INDAHSARI KUSUMA DEWI*, LUQMAN BUCHORI AND AJI PRASETYANINGRUM

[1]*Department of Chemical Engineering, Faculty of Engineering, Universitas Diponegoro, Jl. Prof. H. Soedarto S.H., Semarang 50275, Indonesia*

**Corresponding author: ndah.dewi17@gmail.com*

(Received: 14 January 2023; Accepted: 4 April 2023; Published on-line: 4 July 2023)

ABSTRACT: Oil palm mesocarp fiber is a promising lignocellulosic biomass as a raw material for valorizing biomass into more valuable products such as second-generation biofuels, biocomposites, or bioenergy. However, the lignin composition present in lignocellulosic biomass provides resistance to the valorization process and protects the cellulose composition, thereby limiting the conversion of cellulose into more valuable products. The hybrid ozonation-ultrasonic method as a lignin-degrading method is starting to be considered an effective method. Additionally, a Box-Behnken Design (BBD) was employed to investigate each independent variable's effect on pretreatment process conditions using the response surface methodology (RSM), namely reaction time (30-90) min, reaction temperature (20 -40) ºC and ozone flow rate (1-3) L/min to the response of the percentage of lignin degradation (%). The optimum condition of the pretreatment process is determined using the desirability function graph. The results showed that reaction time, reaction temperature, and ozone flow rate had a significant effect on lignin degradation ($p < 0.05$). The optimum conditions obtained the highest percentage of lignin degradation, namely 92.08% at a reaction temperature of 30 ºC with an ozone flow rate of 2 L/min for 60 minutes reaction time. The decrease in lignin absorption peaks at 1638 cm^{-1} and 1427 cm^{-1} was supported by the results of the analysis of increased crystallinity in the sample after the pretreatment of lignin degradation to 80.20% and was validated by changes in the morphology of the mesocarp fiber after the pretreatment process indicating that the lignin compound had been successfully degraded from cellulose products of mesocarp fibers.

ABSTRAK: Sabut gentian kelapa sawit berpotensi sebagai bahan mentah biojisim lignoselulosa bagi menambah nilai produk biojisim seperti bahan bio api generasi kedua, biokomposit atau biotenaga. Walau bagaimanapun, komposisi lignin yang wujud dalam biojisim lignoselulosa menentang proses tambah nilai dan melindungi komposisi selulosa, dengan itu mengehadkan penukaran selulosa kepada produk yang lebih berharga. Kaedah hibrid ozonasi-ultrasonik sebagai kaedah merendahkan lignin, mula mendapat perhatian sebagai kaedah berkesan. Selain itu, Reka Bentuk Kotak-Behnken (BBD) telah digunakan bagi menyiasat setiap kesan pembolehubah bebas pada keadaan proses prarawatan menggunakan kaedah permukaan tindak balas (RSM), iaitu masa tindak balas (30-90) min, suhu tindak balas (20 -40) ºC dan kadar aliran ozon (1-3) L/min terhadap tindak balas pada peratusan degradasi lignin (%). Keadaan optimum bagi proses prarawatan ditentukan menggunakan graf fungsi keboleh inginan. Dapatan kajian menunjukkan bahawa masa tindak balas, suhu tindak balas, dan kadar aliran ozon mempunyai kesan yang signifikan terhadap degradasi lignin ($p<0.05$). Keadaan optimum peratusan degradasi lignin tertinggi adalah pada 92.08% pada suhu tindak balas 30 ºC dengan kadar aliran ozon 2 L/min selama 60 minit masa tindak balas. Penurunan puncak penyerapan lignin pada 1638 cm^{-1} dan 1427 cm^{-1} disokong

oleh keputusan analisis peningkatan kehabluran sampel selepas prarawatan degradasi lignin sebanyak 80.20% dan telah disahkan oleh perubahan morfologi sabut gentian selepas proses prarawatan menunjukkan bahawa sebatian lignin telah berjaya didegradasi daripada produk selulosa sabut gentian.

KEY WORDS: *Hybrid ozonation-ultrasonic lignin degradation, oil palm mesocarp fiber, RSM, AOPs pretreatment*

1. INTRODUCTION

Mesocarp fiber is one of the by-products produced in large quantities by the palm oil industry in the palm oil production process. Total palm oil production continues to increase yearly due to the increasing world market demand for vegetable oil. In 2020, the total world palm oil production reached 73 million tonnes per year, then it will increase in the following year 2021 to reach 75 million tonnes per year, and now the total worldwide palm oil production has reached 77 to 79 million tonnes per year [1,2,3]. Then, from the total amount of palm oil production, it produces around 12-15% by-products in the form of mesocarp fiber which, if not handled seriously, can become a problem in waste management and endanger the surrounding environment [4]. In line with the problems that can be caused, oil palm mesocarp fiber is also one of the interesting potential lignocellulosic biomasses because of its abundant availability at a low cost. It has a high main component of cellulose which is around 40.12% by weight, hemicellulose 20.12% by weight, and 30.33% lignin by weight, so if utilized properly, it can be promising in terms of the economy [5,6,7,8].

The valorization of oil palm mesocarp fiber biomass, which entails converting lignocellulosic biomass into second-generation biofuels or other valuable products such as biocomposites, has become a current trend. However, the complex structure of lignocellulosic biomass has received special attention because of the lignin component that hinders the accessibility of cellulose, thereby inhibiting the valorization of lignocellulosic biomass [9]. Therefore, the pretreatment process is an important step before valorizing lignocellulosic biomass. The pretreatment process's primary goal is to degrade the complex structure of lignocellulosic biomass into simpler fibrous components and remove some of the lignin components in what is commonly referred to as the biomass delignification process [10]. Ozone-based advanced oxidation technology is one of the oxidation methods that has recently gained popularity for degrading complex compounds in waste and biomass [11]. In degrading complex compounds effectively and optimally, advanced ozone-based oxidation technology is based on the use of radical generation such as the hydroxyl radical (OH^*) as an oxidizing agent which has a strong oxidation potential value and is non-selective so that it shows good potential in the treatment of lignocellulosic biomass [12,13].

Ozone-based advanced oxidation processes (AOPs) can degrade complex compounds by two mechanisms that depend on the pH of different solutions, namely directly and indirectly. The indirect oxidation of ozone involves the hydroxyl radical (OH^*) as an oxidizing agent, while the direct oxidation of ozone represents oxidation with ozone molecules [14]. Both ozone-based advanced oxidation processes rely on different pH solutions to react with complex compounds. Ozone oxidation directly oxidizes complex compounds when the pH of the solution is acidic (< 5), while indirect ozone oxidation can take place when the pH of the solution is alkaline (> 8) [15]. The oxidation potential of ozone is 2.07 eV, which makes it a selective and strong oxidizer [11,14]. The ozonation process as a pretreatment method for lignocellulosic biomass has several advantages, such as a strong oxidation potential value and a characteristic of ozone molecules that they react readily with conjugated double bonds found

in complex compounds and functional groups with high density, which makes ozone able to oxidize lignin which has a high C=C bond [16]. In addition, ozone can be easily decomposed into compounds with greater oxidizing abilities, such as hydroxyl radicals (OH^*), which have a potential oxidation value of 2.80 eV and are also non-selective so that they can easily be better in degrading complex compounds of lignocellulosic biomass [11].

Ozonation is also a green pretreatment method because, in the process of oxidizing lignocellulosic biomass, it does not produce side products that can harm the surrounding environment. Ozone can decompose into oxygen molecules, so it is safe if directly discharged into the surrounding environment. The filtrate produced from the lignin degradation process can be utilized for lignin recovery [17]. Praptyana and Budiyono [18] reported that the pretreatment of mahogany sawdust biomass using ozone in alkaline conditions could degrade lignin and increase biohydrogen production up to 86.9% over other pretreatments. Similar results were also reported by Hassan et al. [19], that ozone pre-treatment of green algae Ulva lactuca could degrade complex biomass compounds, thereby significantly increasing biogas production. In addition, ozone has a few drawbacks that limit its industrial use, which is related to the insufficient solubility and stability of ozone molecules in solution and their limited selectivity in the oxidation process resulting in the low mass transfer of ozone in solution [20,21].

In recent years, researchers have become interested in finding ways to improve ozone mass transfer. The ultrasonic process provides several advantages compared to other technologies in increasing the efficiency of ozone-based advanced oxidation processes (AOPs), which include a simple operational process that can increase the solubility of ozone and does not produce harmful pollutants [22]. Several studies have found that ultrasonic cavitation has the ability to increase the mass transfer of ozone in water and also increase the production of free radicals such as hydroxyl radicals (OH^*). This is because the cavitation phenomenon in the ultrasonic process can cause the formation, growth, and collapse of acoustic bubbles, which can produce great energy with very high temperatures (> 4000 K) and local pressure (> 500 bar) as a result of the hotspot phenomenon that is formed when the rupture cavitation bubbles to increase the surface area of contact between ozone and solution and can cause dissociation of water molecules which leads to an increase in the mass transfer of ozone and an increase in the formation of radical compounds such as hydroxyl radicals (OH^*) [23]. The hybrid of ozonation and ultrasonic methods can accelerate the oxidation process of lignin by hydroxyl radical compounds (OH^*) into oxyaromatics compounds, which then turn into short-chain aliphatic acids. Additionally, the collapse of cavitation bubbles in the ultrasonic process also produces hydromechanical shear forces in solution which can interfere with Surface morphology of lignocellulosic biomass [24]. The synergistic effect between the ozonation and ultrasonic processes can be described as follows [25].

Shen et al. [26] investigated the effectiveness of using ozonation and ultrasonic processes simultaneously to provide a significant degradation effect of X-3B reactive red dye up to 99.2%. In addition, Weavers and Hoffmann [27] also reported that the mass transfer of ozone was much larger at a frequency of 20 kHz, which resulted in a mass transfer coefficient value (K_La 0.28 – 0.41 min^{-1}), while at a frequency of 500 kHz, the value of the displacement coefficient was mass is only equal to (K_La 0.05 – 0.1 $minutes^{-1}$). Therefore, the combination of ozonation and ultrasonic processes is an approach that has great potential and promise. The synergistic effect of the combination of the two processes increases the efficiency of the degradation of complex compounds such as lignocellulosic biomass. In line with the synergistic effect of the hybrid ozonation-ultrasonic method, process variables also affect the effectiveness of the lignocellulosic biomass pretreatment process. Optimization of the hybrid ozonation-

ultrasonic process variables using statistical and mathematical approaches such as the Response Surface Methodology (RSM) method in the biomass pretreatment process have not been reported so far.

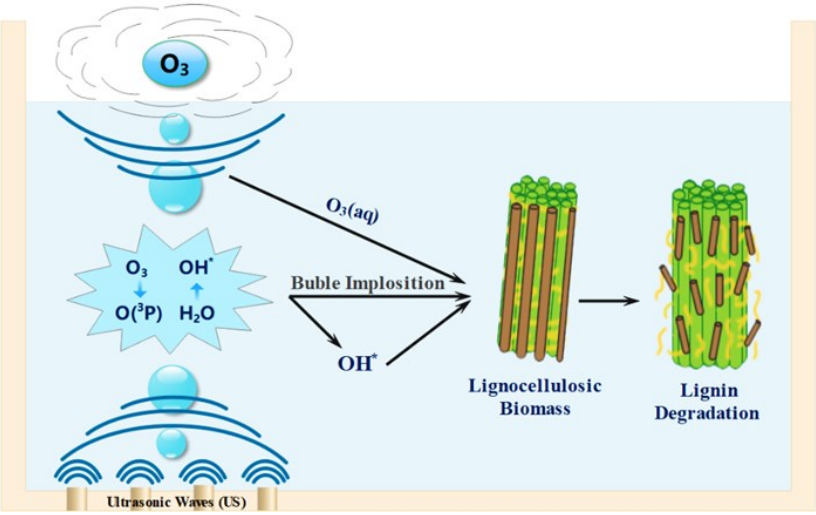

Fig. 1. Synergism of hybrid ozonation-ultrasonic pretreatment

Thus, it is necessary to optimize the process variables to provide information about the effect of the pretreatment process variables on the response, namely lignin degradation, and to save processing time and pretreatment costs [5]. This study applied a hybrid ozonation-ultrasonic process as a pretreatment method for lignocellulosic biomass in oil palm mesocarp fibers. Three different operational variables, operating temperature, operating time, and ozone flow rate were evaluated using a three-factor box-behnken design (BBD) approach, which is one type of design of experiment (DOE) in the response surface methodology (RSM) method to determine the most influential variable on the response and to obtain optimal operating conditions in the biomass pretreatment process.

2. EXPERIMENT

2.1. Material and Methods

The oil palm mesocarp fibers in this study were obtained from Indonesian palm oil companies. Mesocarp fiber raw materials were washed with water to remove particulates and dried in an oven at 105 ºC for 24 hours. Then the size was made uniform at 60 mesh and stored in a closed container at room temperature. The chemicals used in this study were H_2SO_4 with a purity of 95% - 97% (E. Merck Cat No. 100731), NaOH with a purity of 99% (E. Merck Cat. No. 106498), ozone gas obtained from an ozone generator (Dipo Technology Indonesia) and ultrasonic irradiation was carried out using an ultrasonic bath type KLS 303365 equipped with a thermostatic water bath with a frequency of 42 kHz.

2.2. Oil Palm Mesocarp Fiber (OPMF) Characterization

The characterization of the composition of cellulose and hemicellulose in oil palm mesocarp fibers was determined by the cellulose isolation and bleaching methods that were slightly modified from Candido [28]. While the characterization of lignin composition in oil palm mesocarp fibers was determined using the Chesson Datta method, namely by weighing 1 g of dry sample (weight a), then reacting with 150 mL of distilled water for 1 hour at a temperature of 100 ºC. The resulting residue was then washed with hot aquadest, dried in an

oven for 24 hours, and weighed to a constant (weight b). Then the solid was reacted again with 150 mL H_2SO_4 1N for 1 hour at 100 ºC, filtered and washed with distilled water, dried in the oven for 24 hours at 100 ºC, and then weighed to a constant (weight c). The weighed solid was then reacted again with 10 mL of 72% H_2SO_4 for 4 hours at room temperature, then added to 150 mL of 1N H_2SO_4 and the mixture was refluxed for 1 hour. The residue was washed, dried, and weighed to a constant weight (weight d). Following that, the final solid is subjected to dry ashing using a muffle furnace at 525 ºC, and the dry ash resulting from that process is weighed until constant (weight e). The percentage composition of cellulose, hemicellulose and lignin can be calculated by equations (1 - 4). Changes in the mesocarp fiber surface morphology were confirmed using Scanning Electron Microscopy (SEM). In contrast, the crystallinity value of the OPMF before pretreatment and after pretreatment was confirmed by X-Ray Diffraction (XRD) rays, and the change in the chemical structure after the pretreatment process was confirmed by using Fourier-Transform Infrared Spectroscopy (FTIR).

$$Cellulose \quad (\%) = \left[\frac{c-d}{a}\right] \times 100\% \tag{1}$$

$$Hemicellulose \quad (\%) = \left[\frac{b-c}{a}\right] \times 100\% \tag{2}$$

$$Lignin \quad (\%) = \left[\frac{d-e}{a}\right] \times 100\% \tag{3}$$

$$Lignin\ Degradation(\%) = \left[\frac{lignin\ before\ pretreatment - lignin\ after\ pretreatment}{lignin\ before\ pretreatment}\right] \times 100\% \tag{4}$$

In which *a* represents the initial dry weight (g) of the oil palm fiber sample, *b* represents the dry weight of the sample residue after refluxing with hot aquadest (g), *c* represents the weight of sample residue after refluxing with H_2SO_4 1 N (g), *d* represents the weight of sample residue after 72% H_2SO_4 treatment (g), and *e* represents the weight of ash from sample residue (g).

2.3. Hybrid Ozonation-Ultrasonic Pretreatment

The hybrid ozonation-ultrasonic pretreatment process for oil palm mesocarp fibers was carried out using a glass reactor equipped with a gas sparger and an ultrasound bath, as shown in Fig 2.

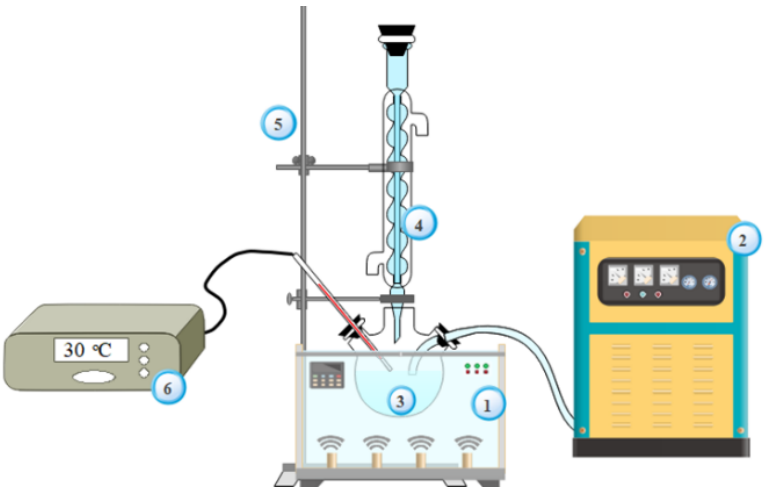

Fig. 2. Hybrid ozonation-ultrasonic process equipment, (1) ultrasound bath; (2) ozone generator; (3) flask; (4) reverse cooling; (5) stative clamp; (6) thermocouple

Oil palm mesocarp fibers weighing 15 g were placed into a glass reactor connected to an ozone generator and ultrasound bath, then 225 mL of distilled water was added, which was adjusted to pH 9 by adding 0.1 M NaOH solution, and the reaction process was carried out by flowing ozone gas and ultrasonic irradiation at an intensity of 42 kHz. After the reaction process is complete, the ultrasound bath and ozone generator were turned off, and the reaction products were filtered and then washed with distilled water until the pH was neutral. The filtered residue was dried using an oven at 105 ºC for 24 hours and then stored for analysis of the composition of lignin, hemicellulose, and cellulose using the Chesson-Datta method.

2.4.Process Variable Optimization

Experimental analysis of the mesocarp fiber pretreatment optimization process was carried out using statistical software 6.0 with RSM and BBD design, which has three factors, one block, and fifteen trials, was chosen to identify the optimal parameters that have a significant influence on the response and investigate the optimum conditions for the pretreatment process of oil palm mesocarp fibers [29]. Three independent variables in the pretreatment process, namely reaction time (X_1), reaction temperature (X_2), and ozone flow rate (X_3), each of which has three levels of value, were selected based on Abdurrahman [25]. The ranges of independent variables in the experimental process are summarized in Table 1, while the experimental designs given by the RSM are presented in Table 2.

Table 1: Process independent variable range

Variable	Variable Code				Response (%)
	Code	-1	0	+1	
Reaction time (min)	x_1	30	60	90	Lignin Degradation
Reaction Temperature (ºC)	x_2	20	30	40	
Ozone Flow Rate (L/min)	x_3	1	2	3	

Table 2: Independent variable from design of experiment (DOE)

Run	Variable			Code			Response
	Time (min)	Temperature (ºC)	Ozone Flow Rate (L/min)	X_1	X_2	X_3	Lignin Degradation (%)
1	30	20	2	-1	-1	0	Y_1
2	90	20	2	1	-1	0	Y_2
3	30	40	2	-1	1	0	Y_3
4	90	40	2	1	1	0	Y_4
5	30	30	1	-1	0	-1	Y_5
6	90	30	1	1	0	-1	Y_6
7	30	30	3	-1	0	1	Y_7
8	90	30	3	1	0	1	Y_8
9	60	20	1	0	-1	-1	Y_9
10	60	40	1	0	1	-1	Y_{10}
11	60	20	3	0	-1	1	Y_{11}
12	60	40	3	0	1	1	Y_{12}
13	60	30	2	0	0	0	Y_{13}
14	60	30	2	0	0	0	Y_{14}
15	60	30	2	0	0	0	Y_{15}

The data obtained were analyzed using analysis of variance (ANOVA) and the response surface to determine the functional relationship between the independent process variables and the desired response [30]. The second-order polynomial regression equation describes the significance of the relationship between the independent variables in the response. The polynomial equation is described as follows:

$$Y = \beta_0 + \sum_{i=1}^{k} \beta_i X_i + \sum_{i=1}^{k} \beta_{ii} X_i^2 + \sum_{i=1}^{k} \sum_{j=i+1}^{k} \beta_{ij} X_i X_j \quad (5)$$

Where Y is the desired response, β_O represents a constant coefficient, X_i and X_j represent independent variables, k represents the number of independent variables, and β_i, β_{ii}, and β_{ij} represent linear coefficients, quadratic coefficients, and interaction coefficients. Using the RSM method in the experimental process can help summarize the number of trials needed to optimize the system and response so that the optimization process can be more efficient and save the cost of the experiments used [31].

2.5.Analysis of Cellulose Crystallinity with X-Ray Diffraction (XRD)

Crystallinity index (CrI) values of oil palm mesocarp fiber biomass without pretreatment and pretreatment and commercial cellulose were analyzed using X-rays at an angle of 2θ ranging from 5° to 100°. The detector detects the recorded X-ray diffraction spectrum results to form a diffraction pattern with peak intensity, which can be used to calculate cellulose crystallinity. The crystallinity index (CrI) value can be calculated using the following methods [32].

$$CRI\ (\%) = \left(\frac{I_{002} - I_{am}}{I_{002}}\right) \times 100 \quad (6)$$

Where (I_{002}) denotes the crystal peak intensity, (CrI) the crystallinity index, and (I_{am}) the amorphous phase peak intensity.

2.6. Functional Group Analysis with Fourier-Transform Infrared Spectroscopy (FTIR)

Fourier-transform infrared spectroscopy (FTIR) analysis aims to determine the chemical composition of lignocellulosic biomass of oil palm mesocarp fiber before pretreatment and after pretreatment with commercial cellulose composition as the standard value. Infrared spectroscopy (FTIR) examination of lignocellulosic biomass was performed at wavelengths between 400 cm^{-1} and 4000 cm^{-1}. The results of all formed spectra are reported in reflection mode at a predetermined wavelength range.

2.7.Cellulose Morphology Analysis by Scanning Electron Microscopy (SEM)

In order to study how the oil palm mesocarp fiber changed morphologically before and after pretreatment with lignin degradation, scanning electron microscopy (SEM) was conducted. Micrographs of oil palm mesocarp fiber biomass samples were observed at 7500 x magnification.

3. RESULTS AND DISCUSSION

3.1. Oil Palm Mesocarp Fiber Composition

The main composition of oil palm mesocarp fiber consists of carbohydrates, namely holocellulose (cellulose and hemicellulose) and lignin. Oil palm mesocarp fiber composition can be determined using the Chesson-Datta method. The results of measurements using the

Chesson Datta method show that the composition of the oil palm mesocarp fiber in this study is in accordance with previous studies that have been reported in the literature (Table 3). The lignin composition in mesocarp fiber, which is relatively high, gives toughness and stiffness to the cell walls of biomass so that it can become an obstacle in the valorization process of oil palm mesocarp fiber biomass both in the bioenergy and biocomposite fields [33].

Table 3. Composition of treated and untreated oil palm mesocarp fiber

Raw material	Oil Palm Mesocarp Fiber Composition (%)			Reference
	Cellulose	Hemicellulose	Lignin	
Untreated Mesocarp Fiber	37.12	29.72	28.70	This study
Untreated Mesocarp Fiber	43.70	34.20	24.00	[34]
Untreated Mesocarp Fiber	28.28	32.70	32.40	[35]
Untreated Mesocarp Fiber	27.85	24.04	31.30	[36]
Treated Mesocarp Fiber	90.01	4.56	2.27	This study

From the data reported, the composition of lignin in oil palm mesocarp fibers is relatively different. It is influenced by differences in the background from plantation areas and types of oil palm as well as the level of maturity of oil palm fruit when the sample is used [37]. Therefore, it is very important to analyze the initial composition of lignocellulosic biomass to determine the composition of the raw materials to be used, considering that cellulose, hemicellulose, and lignin are the main compositions that can affect the efficiency in the valorization of oil palm mesocarp fiber biomass. Additionally, the results showed that the lignin and hemicellulose content of palm mesocarp fiber decreased after the hybrid ozonization-ultrasonic pretreatment, as lignin and hemicellulose had been degraded.

3.2. Statistical Analysis and Empirical Models for Lignin Degradation

In this study, the results of the lignin degradation pretreatment and the predicted values generated by the experimental design of the statistical software are shown in Table 4.

The percentage of lignin degradation in mesocarp fiber obtained from this study showed varying values. The lowest percentage of lignin degradation was obtained at 79.27%, and the highest percentage of lignin degradation was obtained at 92.08%. While the process of lignin degradation using the ozonation and ultrasonic methods used individually has been reported by previous studies and shows that lignin degradation is only 87.9% in the ozonation process and 20.11% in the ultrasonic process, respectively [5,38]. Thus, the pretreatment of lignocellulosic biomass using the hybrid ozonation-ultrasonic method showed an increase in the lignin degradation process. Regression analysis uses second-order polynomial equations to explain the relationship between the independent and dependent variables. The polynomial equation is presented in Eqn. (1):

$$Y = 62.3300 + 0.32694\ X_1 + 1.11200\ X_2 + 2.94083\ X_3 - 0.00263\ X_1^2 - 0.01848\ X_2^2 - 0.68833\ X_3^2 + 0.00007\ X_1X_2 - 0.00017\ X_1X_3 - 0.003\ X_2X_3 \quad (1)$$

Where Y is the percentage of lignin degradation (%), X_1 is the time (min), X_2 is the temperature (°C), and X_3 is the ozone flow rate (L/min). The polynomial equation shows that time, temperature, and ozone flow rate can significantly affect the response, namely the percentage of lignin degradation indicated by a positive constant value in the model. Meanwhile, the interaction between the independent variables did not significantly affect the

percentage of lignin degradation. It was reflected in the negative value of the model. The significance of the polynomial equation can be validated by the resulting regression coefficient (R^2) and statistical analysis such as analysis of variance (ANOVA). The regression coefficient value formed from this study is 99.86%. It proves that the predicted and observed values are close together, so the model can be represented in predicting lignin degradation with an error value of less than 5%. The significance of the independent variables of the hybrid ozonation-ultrasonic pretreatment consisting of reaction time, reaction temperature, and ozone flow rate to the response, namely the percentage of lignin degradation, is shown in Table 5.

Table 4: Experimental data of oil palm mesocarp fiber

Run	Variable			Response (%)	
	Time (min)	Temperature (°C)	Ozone Flow Rate (L/min)	Experiment	Prediction
1	30	20	2	87.55	87.60
2	90	20	2	88.24	88.25
3	30	40	2	87.51	87.50
4	90	40	2	88.12	88.07
5	30	30	1	88.64	88.61
6	90	30	1	89.20	89.21
7	30	30	3	88.82	88.81
8	90	30	3	89.40	89.43
9	60	20	1	89.48	89.46
10	60	40	1	89.34	89.38
11	60	20	3	89.78	89.74
12	60	40	3	89.52	89.54
13	60	30	2	92.08	92.07
14	60	30	2	92.06	92.07
15	60	30	2	92.07	92.07

P values (probability) can be used to differentiate statistical analysis results in ANOVA tables. Where if the value of P (probability) obtained is less than 5% or ($P < 0.05$), then it is considered significant because it has a probability level of 95%. It can be inferred that the independent variable and response have a greater significance if the P value (probability) is smaller [39]. Statistical analysis in this study showed that the linear function and quadratic function of the variable reaction time (X_1), reaction temperature (X_2), and ozone flow rate (X_3) showed a significant effect on the response of the percentage of lignin degradation because it had a P value <0.05. The interaction function between the reaction time variable and the ozone flow rate (X_1X_3) showed similar P value. Meanwhile, the interaction function between the variable reaction time and reaction temperature (X_1X_2) and the reaction temperature variable and ozone flow rate (X_2X_3) did not have a significant effect on the response ($P > 0.05$). This hypothesis is strengthened by the F-test (Fisher), where the results obtained from the F-test show that the independent variables (reaction time, reaction temperature, and ozone flow rate), both in linear and quadratic form, have a higher F value than the F table (F-value > 4.772) so that it can be said that the independent variables in the linear and quadratic forms have a significant effect on lignin degradation. In the interaction between variables, the F-value has a smaller value than the F-table (F-value < 4.772), so the interaction between variables does not have a significant effect on lignin degradation.

Table 5: ANOVA for quadratic equation model in hybrid ozonation-ultrasonic pretreatment

Source	*df*	*SS*	*MS*	Reg Coeff	P-Value	F-Value	
Model	9	32.3804	3.5978	62.3300	0.00000	1484.660	Significant
Time (X_1)	1	0.7442	0.7442	0.32694	0.00001	307.098	
Temperature (X_2)	1	0.0392	0.0392	1.11200	0.01010	16.176	
Ozone Flow Rate (X_3)	1	0.0925	0.0925	2.94083	0.00162	38.150	
Time (X_1^2)	1	20.6228	20.6228	-0.00263	0.00000	8510.101	
Temperature ($X_2^{2)}$	1	12.6142	12.6142	-0.01848	0.00000	5205.295	
Ozone Flow Rate (X_3^2)	1	1.7494	1.7494	-0.68833	0.00000	721.909	
Time-Temperature (X_1X_2)	1	0.0016	0.0016	-0.00007	0.45341	0.660	Not Significant
Time- Flow Rate (X_1X_3)	1	0.0001	0.0001	0.00017	0.84703	0.041	
Temperature- Flow Rate (X_2X_3)	1	0.0036	0.0036	-0.00300	0.27727	1.486	
Error	5	0.0121	0.0024				
Lack-of-Fit	3	0.0117	0.0039		0.0572		
Pure Error	2	0.0005	0.0002				
Total	14	32.3925					
$R^2 = 0.9996$ dan $R^2_{Adj} = 0.9989$							

The residual mean square (MS) value in the analysis of variance (ANOVA) is used to describe the difference between the experimental data and the predicted value of the model [40]. This study produced a residual mean square (MS) value of 0.0173, so it can be concluded that the model used is good enough and accurate in explaining the closeness between the experimental results and the predicted values obtained from the experimental design. The closeness between the experimental data and the predicted value is clarified by the coefficient

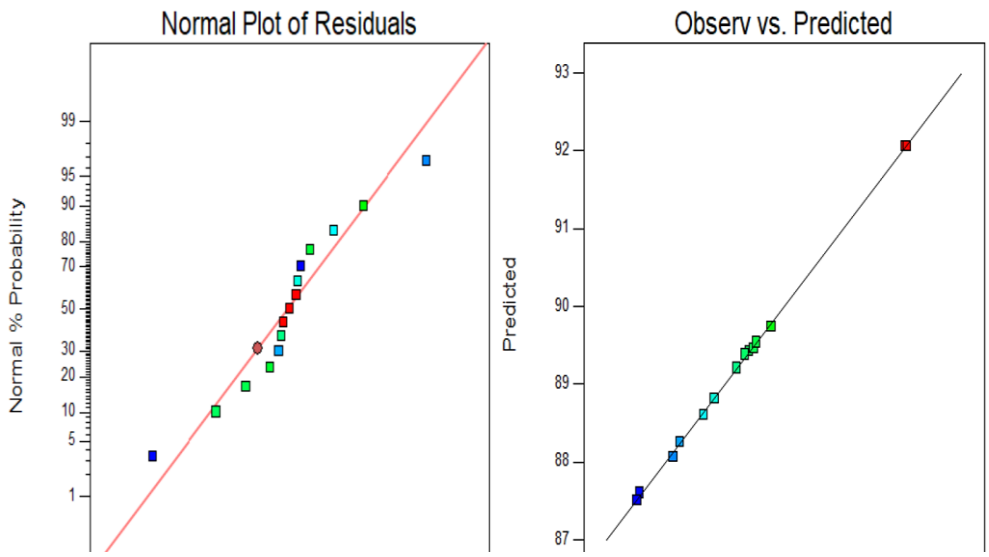

Fig. 3. Probability plots (a) normal vs internally studentized residual, (b) predicted vs observer

of determination (R^2) obtained, which is equal to 0.9996, so it can be stated that 99.96% of the model can explain the experimental data. The reliability and significance of the model can be validated by looking at the average probability percentage in Figure 3a and the relationship between the experimental results obtained, and the predicted value of the model can also be validated by the observer vs predicted diagram illustrated in Figure 3b.

The diagonal line on the normal probability plot shows the data predicted by the experimental design. In contrast, the dots around the diagonal line show the value of the experimental results obtained. The closer the points, which are the experimental data, to the diagonal line, the residual values are normally distributed [41]. This normal distribution analysis aims to observe the magnitude of the deviation from the model. In this study, the normal probability plot shows dots that spread and approach the diagonal line, so it can be said that the model given by the experimental design can fulfill the assumption of normality.

3.3.Effect and Interaction of Variables Process on Lignin Degradation

The influence of process variables and their interactions during the pretreatment of lignin degradation with the ultrasonic hybrid ozonation method can be explained by employing response surface plots. Response surface analysis can provide a 3-dimensional profile that explains the relationship between the independent variables and the response. The response surface plot of the percentage of lignin degradation is presented in Figure 4.

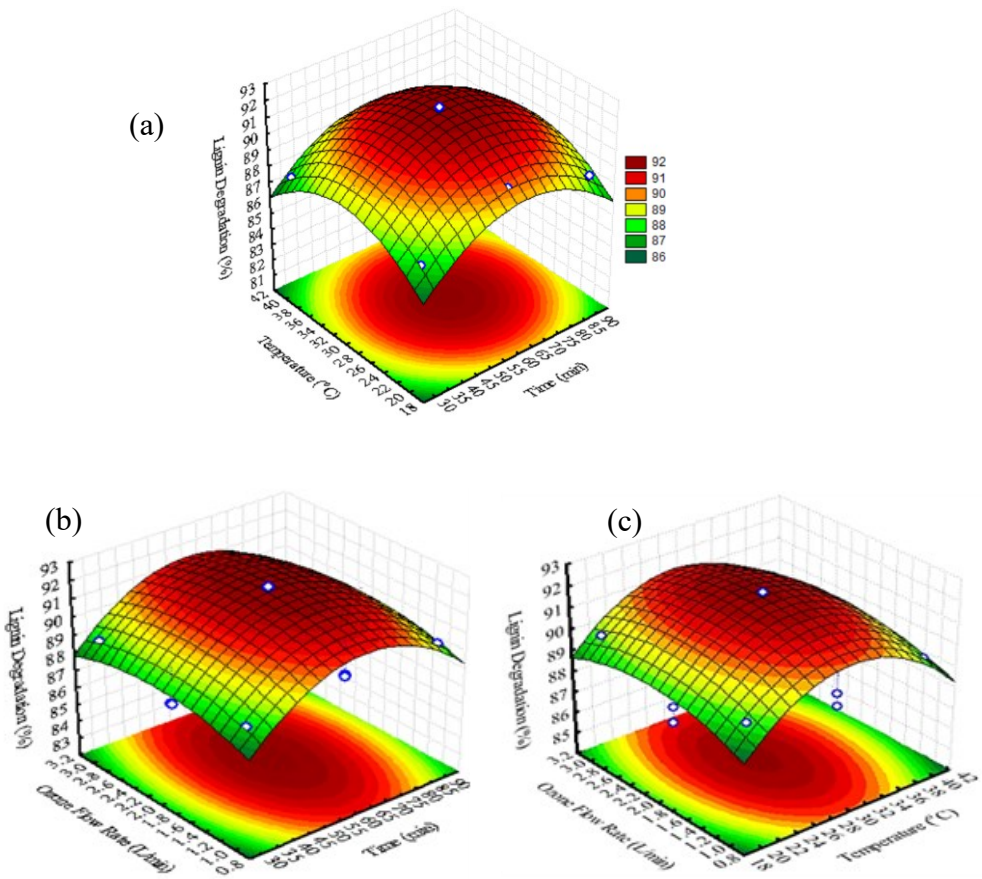

Fig. 4. Response surface methodology of an hybrid ozonation-ultrasonic pretreatment (a) X_1 & X_2, (b) X_1 & X_3, (c) X_2 & X_3

Based on the response surface plot images, the percentage of lignin degradation increases with increasing reaction time, reaction temperature, and ozone flow rate up to a certain critical point. The highest percentage of lignin degradation is represented by the contour plot area of the response surface, which has a solid red color. In contrast, the smallest percentage of lignin degradation depicted on the contour plot is colored green. In this study, the contour plots showed that more than 90% of lignin degradation was obtained when it was reacted at a temperature of 24-31 ºC, with an ozone flow rate of 1-2 L/minute, for 50-65 minutes. According to Ramados et al. [42] and Pujakaroni et al. [43], the highest percentage of lignin degradation occurs when the temperature is 40 ºC for 60 minutes. Increasing the reaction time can extend the contact time between radical compounds and a little ozone with lignocellulosic biomass, thus increasing lignin degradation. However, using a reaction time of more than 60 minutes does not have a significant effect because most of the lignin has been degraded so that it opens the surface of lignocellulosic biomass, and ozone could attack the holocellulose component [44]. Likewise, an increase in temperature causes an increase in the solubility and diffusion coefficient of the lignin component. On the other hand, although the concentration and solubility of ozone in water decrease with an increase in the reaction temperature, more hydroxy radical compounds are also produced under the same conditions, which have a greater oxidation potential value than ozone so that they are more oxidative which leads to an increase in the rate of degradation [45].

According to Chiha et al. [46], the degradation products increased from 20°C to 30°C as temperature increased and tended to be constant and even decreased when the temperature was higher than 30 ºC. The decrease in the efficiency of the organic compound degradation process using the hybrid ozonation-ultrasonic method is caused by a decrease in ozone solubility and a decrease in the formation of radical compounds due to an increase in water vapor in the bubbles, which provides a cushioning effect on the collapsed bubbles so that the bursting of cavitation bubbles only produces low energy [47]. A flow rate of 2 L/min of ozone has a significant influence on the results, as shown by Wang et al. [48], that the ozone flow rate is increased, and degradation efficiency increases because cavitation bubbles form under ultrasonic irradiation, accelerating the mass transfer of ozone and causing radical compounds to form that can accelerate organic compound degradation. However, excessive ozone flow rates can cause greater turbulence, decreasing the contact time between ozone and water and shorter biomass, thereby reducing the degradation percentage [49].

3.4.Optimization of The Hybrid Ozonation-Ultrasonic Pretreatment Process Variables

Optimizing the lignin degradation pretreatment process using the hybrid ozonation-ultrasonic method was conducted by analyzing the desirability function represented by the response desirability profiling contained in statistical software 6. This tool consists of a series of graphs that represent every independent variable to determine whether the independent variables provide significant responses to the desired outcome. The results of optimizing the lignin degradation pretreatment process with the hybrid ozonation-ultrasonic method are shown in Figure 5.

The results of the analysis of the desirability function for each independent variable and the predicted response at optimal conditions can be observed from the response desirability profiling graph. The desirability profile graph shows that the percentage of lignin degradation in the hybrid ozonation-ultrasonic pretreatment has increased along with the increasing values of independent process variables such as reaction time, reaction temperature, and ozone flow rate until they reach a certain critical value. The optimal condition of the lignin degradation process can be seen from the intersection of the independent variables with the highest response values. In this study, the optimum conditions were obtained at 30 ºC, with an ozone flow rate

of 2 L/min, and for 60 minutes of reaction time, the optimum response was in the form of a lignin degradation percentage of 92.08%.

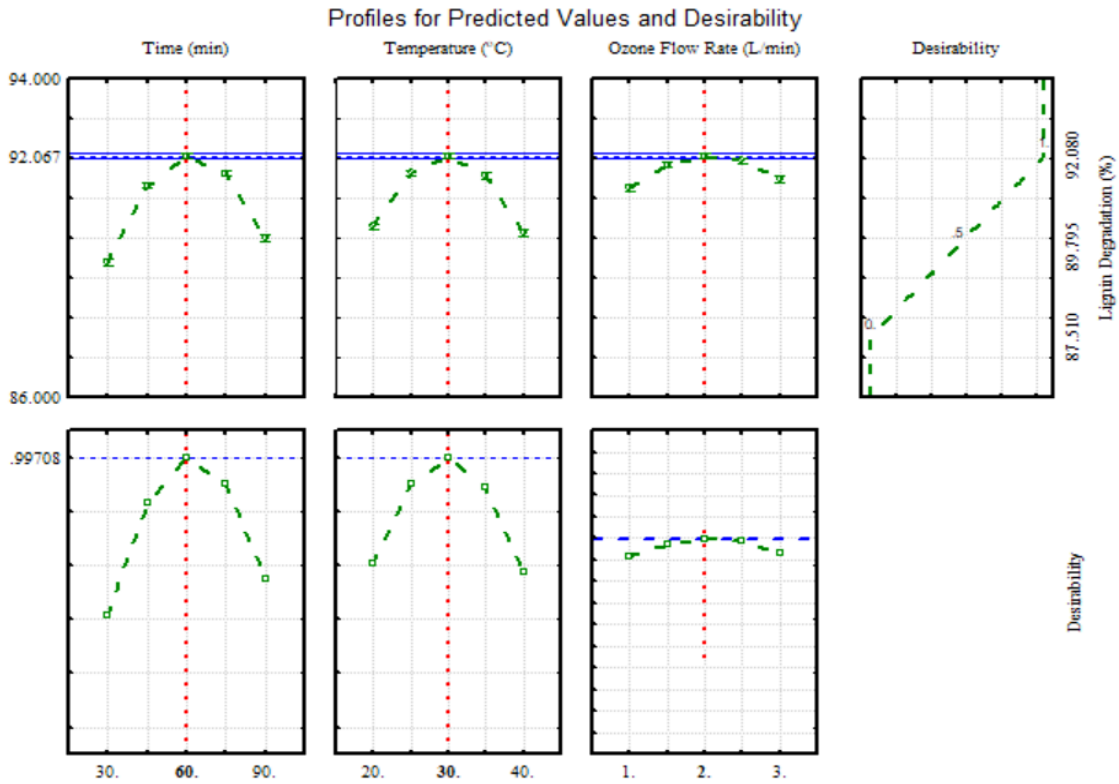

Fig. 5. Profiles desirability of hybrid ozonation-ultrasonic pretreatment

3.5.Proposed Hybrid Ozonation-Ultrasonic Reaction (AOPS) Mechanism

The process of degradation of organic compounds such as lignocellulosic biomass using a combined method of ozonation and ultrasonic processes provides a higher degradation rate than the ozonation and ultrasonic processes when carried out individually. The possible reaction mechanism in the hybrid ozonation-ultrasonic process in degrading lignocellulosic biomass is shown in Figure 6.

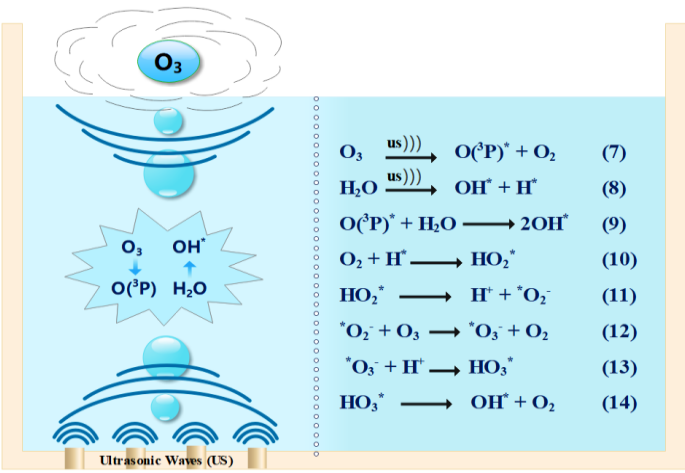

Fig. 6. Reaction mechanism of the hybrid ozonation-ultrasonic pretreatment process for oil palm mesocarp fiber

Decomposed ozone molecules initiate the mechanism of the hybrid ozonation-ultrasonic reaction, and water molecules dissociate in the presence of cavitation bubbles under ultrasonic irradiation to produce the free radical compounds shown in equations (7) and (8), then oxygen atoms produced from the ozone decomposition process. It will react directly with steam from water molecules in the liquid phase to form radical hydroxy compounds, as in equation (9). In addition, a small part of the ozone dissolved during the ultrasonic process can react with lignin directly on lignocellulosic biomass as shown in Figure 7 and then the lignin is degraded. The hybrid ozonation-ultrasonic process generally provides high efficiency in the lignocellulosic biomass pretreatment process because each ozone molecule will produce twice the hydroxyl radicals, which can better oxidize lignin and also the products resulting from the dissociation of water molecules and ozone decomposition will react with each other in the bubble interface and then will diffuse into the aqueous phase (Eq. (10)-(14)) [25]. Zhao et al. [50] reported that the enhanced decomposition of the ozone molecule in the cavitation bubbles under ultrasonic irradiation is due to mechanical effects such as the collapse of the cavitation bubbles.

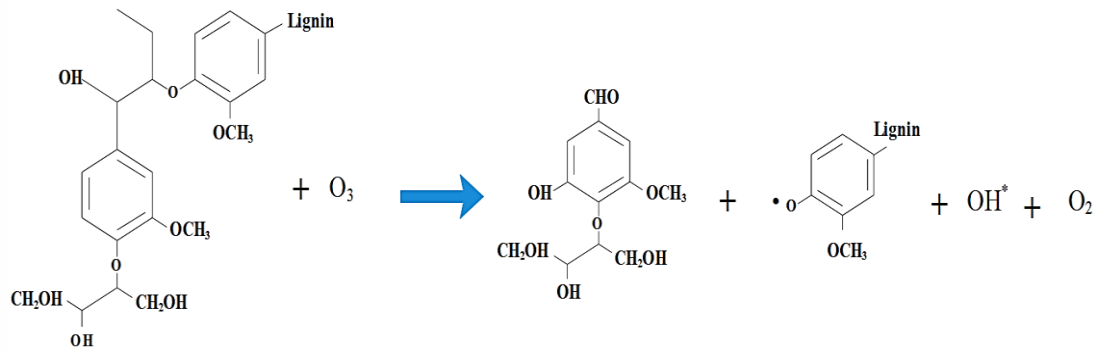

Fig. 7. Mechanism of lignin degradation reaction with ozone

The reaction mechanism for the degradation of lignin compounds by hydroxyl radicals formed during the decomposition process of ozone and the dissociation of water molecules due to the effects of the acoustic cavitation phenomenon in the hybrid ozonation-ultrasonic pretreatment process is shown in Figure 8. However, it is important to note that the mechanism of the proposed lignin degradation reaction by hydroxyl radical compounds is only a speculative mechanism based on the reaction mechanism that has been proposed previously in the literature [51,52]. Pretreatment of lignin degradation with hydroxyl radical compounds involves several processes, such as demethylation or demethoxylation, side chain oxidation, and aromatic hydroxylation processes. Lignin degradation begins with breaking aryl ether bonds in lignin and forms water-soluble phenolic groups [53]. Furthermore, the highly electrophilic hydroxyl radical compounds will also attack other lignin groups rich in electrons through side chain oxidation processes and aromatic hydroxylation.

3.6.X-Ray Diffraction (XRD) Characterization of Lignocellulosic Biomass

XRD analysis of oil palm mesocarp fiber aims to determine the crystal structure of the biomass and structural changes both before and after the lignin degradation process. Cellulose in lignocellulosic biomass has crystalline and amorphous fractions, while the hemicellulose and lignin components have amorphous fractions. The crystallinity index (CrI) can be determined by referring to the XRD pattern, which is the diffraction peak of the cellulose I structure at around 20° and the lowest diffraction peak at around 18°, which is an amorphous cellulose region. Most industries have used analysis of cellulose crystallinity to determine elasticity, absorption, and other physical properties, which are important parameters in the production of biocomposites and bioenergy [54]. The diffraction patterns of non-pretreated and

pretreated oil palm mesocarp fiber biomass and the diffraction patterns of commercial alpha cellulose are presented in Figure 9.

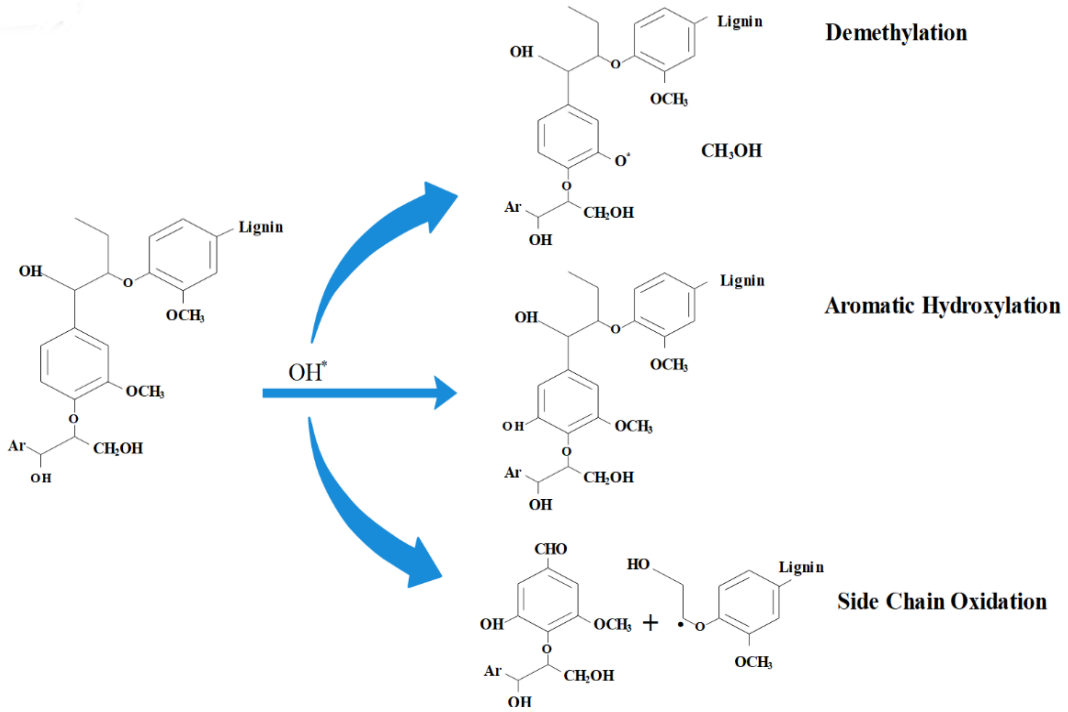

Fig. 8. Mechanism of lignin degradation reaction with hydroxyl radicals

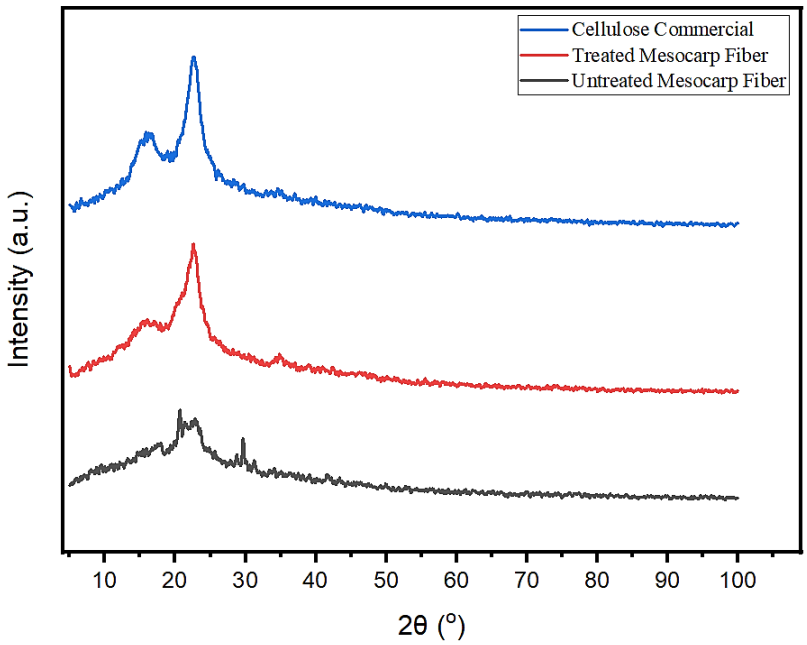

Fig. 9. XRD pattern from untreated and treated oil palm mesocarp fiber

The diffraction peaks detected in the XRD pattern show high peaks at an angle of 2θ, namely at 15° – 16° and 2θ = 20° – 22.5°, which indicates that the oil palm mesocarp fiber biomass has a crystal structure of cellulose I and is a natural plant cellulose [55]. The diffraction peak at angle 2θ, about 22.5°, is associated with the typical peak portion of the cellulose crystal

structure. Whereas at an angle of 2θ, which is 15°, is part of the amorphous region in the biomass. Rosli [56] stated that the diffraction peak of the cellulose crystal structure is at an angle of 2θ, which is around 22-23°. In the biomass that was not pretreated, it showed a broad peak which was associated with the amorphous cellulose area. The crystallinity index (CrI) in mesocarp fibers can be calculated using the Segal method, which is summarized in Table 6.

Table 6: Crystallinity index of oil palm mesocarp fiber and cellulose commercial

Samples	2θ (Amorphous)(°)		2θ (002) (°)		CrI (%)
	Degree	Intensity (I_{am})	Degree	Intensity (I_{002})	
Mesocarp Fiber	20.75	1080	22.67	2332	53.69
Cellulose Hybrid O_3/US	20.33	1250	22.52	6314	80.20
Cellulose Commercial	16.00	2184	22.64	8205	73.38

The crystallinity index (CrI) value of mesocarp fibers undergoing hybrid ultrasonic ozonation pretreatment increased due to the loss of amorphous structures associated with lignin and hemicellulose components. The crystal structure of cellulose is recalcitrant, so it is not easy to remove in the pretreatment process. The low crystallinity index (CrI) value of the raw material for palm oil mesocarp fiber is due to the lignin and hemicellulose components which are cross-linked and have an amorphous structure. Thus, increasing the crystallinity index (CrI) value may imply that pretreatment with the hybrid ozonation-ultrasonic method can degrade components with amorphous structures such as lignin and hemicellulose properly and efficiently. On the other hand, increasing the crystallinity index (CrI) can also encourage an increase in the mechanical properties of cellulose for advanced industrial use [37].

3.7.Fourier-Transform Infrared Spectroscopy (FTIR) Characterization of Biomass

Fourier-transform infrared spectroscopy (FTIR) analysis observed functional groups of oil palm mesocarp fiber before and after hybrid ozonation-ultrasonic pretreatment. The characteristic features of the FTIR spectrum of oil palm mesocarp fiber biomass are presented in Figure 10.

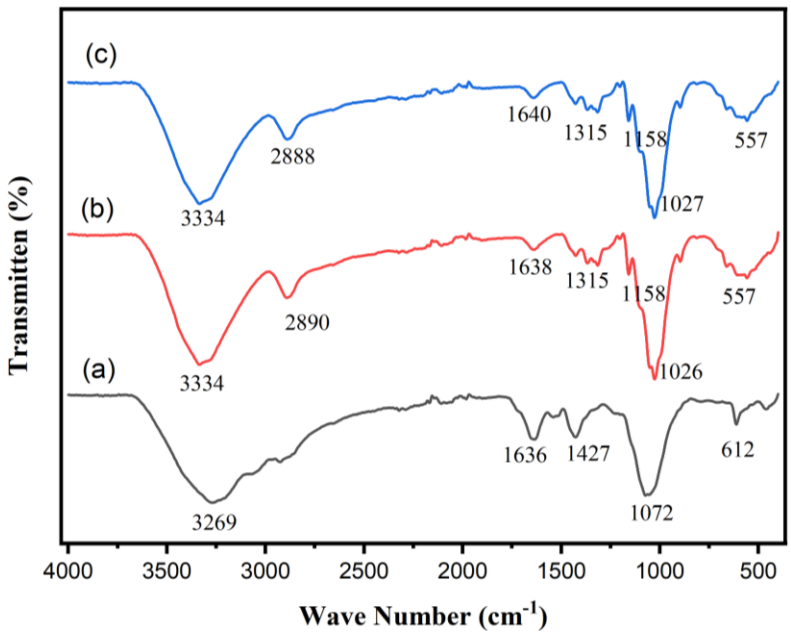

Fig. 10. FTIR spectra of (a) untreated mesocarp fiber; (b) treated mesocarp fiber; (c) commercial cellulose.

The FTIR spectrum of cellulose in oil palm mesocarp fiber both before pretreatment and after pretreatment of lignin degradation produced different types and the number of absorption peaks indicating that the hybrid ozonation-ultrasonic pretreatment could destroy the structure of lignocellulosic biomass. The broad absorption peaks in the region from 3200 cm^{-1} to 3400 cm^{-1} are caused by the stretching of the O-H functional groups, which is the main characterization of cellulose [57,58]. Pretreated cellulose and commercial cellulose samples showed absorption peaks in the area of 2890 cm^{-1}, which indicated sp^3 stretching carbon in the methyl (CH_3) and methylene (CH_2) groups. In contrast, in that area, there were no absorption peaks for non-pretreated oil palm mesocarp fibers [59]. The absorption peaks in the 1638 cm^{-1} area and 1427 cm^{-1} area, respectively, represent the structure of the aromatic ring in lignin according to the C=C and -CH_2 bonding functional groups. The intensity of this absorption peak was reduced in pretreated cellulose and commercial cellulose samples, so it can be concluded that the hybrid ozonation-ultrasonic pretreatment process can damage the structure of lignocellulosic biomass and degrade lignin [60,61]. The absorption peak in the 1315 cm^{-1} area represents a typical cellulose absorption peak with the CH_2 rocking functional group. In this area, the intensity of the absorption peak increases in pretreated cellulose [54,62]. Increased intensity of absorption peaks in pretreated cellulose samples and commercial cellulose also occurs in the areas 1027 cm^{-1} and 557 cm^{-1}, which are the stretching of the β-glycosidic bond, namely C-O-C stretching and the lowest C-H vibration, which refers to an increase in the value of cellulose crystallinity [63,64]. An analysis of Fourier-transform infrared spectroscopy (FTIR) results confirmed that the lignin composition and amorphous areas in lignocellulosic biomass were successfully degraded because similar trends were also shown in commercial cellulose.

3.8. Scanning Electron Microscopy (SEM) Characterization of Biomass

Changes in surface morphology and roughness of the lignocellulosic biomass of oil palm mesocarp fiber before and after pretreatment can be identified through scanning electron

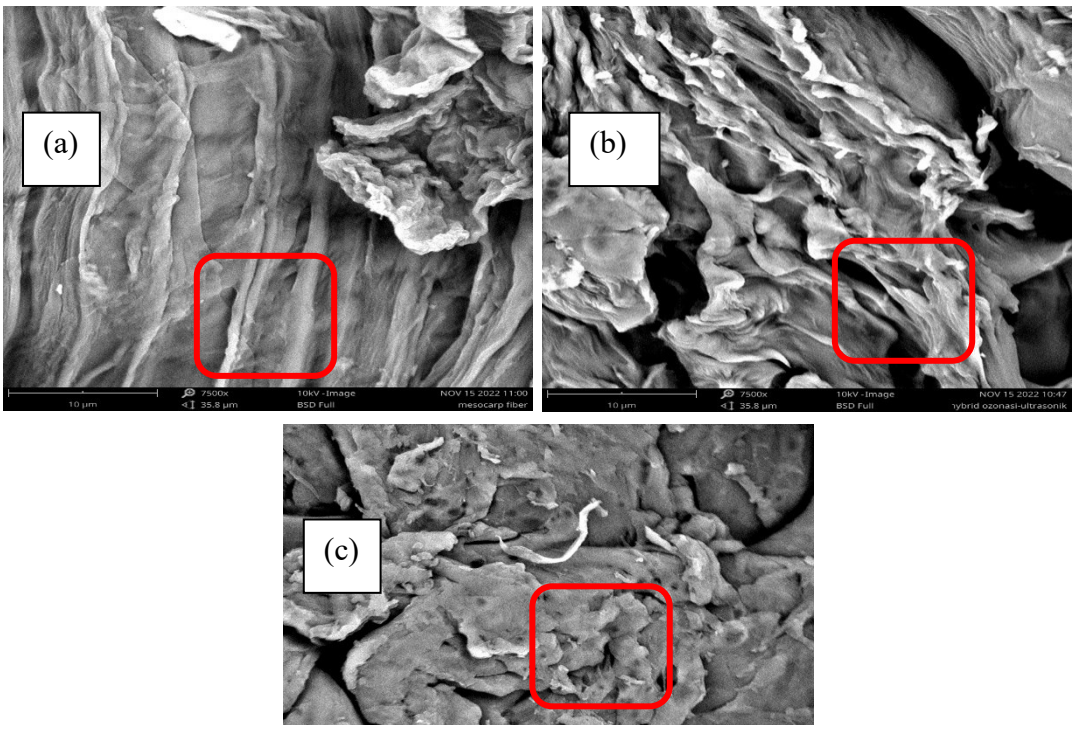

Fig. 11. SEM micrographs of (a) untreated mesocarp fiber, (b) hybrid ozonated-ultrasonic, (c) commercial cellulose

microscopy (SEM) analysis. Micrographs of oil palm mesocarp fibers are presented in Figure 11.

The SEM micrographs demonstrated that the surface of untreated mesocarp fiber lignocellulosic biomass had a dense and smooth structure without any cell wall cracks or fiber damage. It is shown by the red square, which indicates that the lignin structure was still present on the surface of the lignocellulosic biomass. However, in the biomass that was pretreated using the hybrid ozonation-ultrasonic method, as indicated by the red square in section (b), shows that the surface structure of the biomass experienced perforations such as damage caused by some of the degraded lignin structure and also due to shear forces and the sudden burst of cavitation bubbles that collided with the structure. Lignin in the ultrasonic process causes lignocellulosic biomass surface damage [65]. In commercial cellulose, it is also seen that the structure of lignocellulosic biomass is no longer dense and smooth but has been damaged, as shown by the red square in section (c). It is because lignin degradation has occurred, and some of the structure has been removed.

4. CONCLUSION

The hybrid ozonation-ultrasonic pretreatment process for lignin degradation in oil palm mesocarp fiber biomass shows the potential for application, with the acquisition of a high percentage of lignin degradation, up to 98.02%. The RSM was used based on the BBD to obtain the highest percentage of lignin degradation. The optimum conditions were obtained at 30°C, with a flow rate of 2 L/min for 60 minutes. A decrease in the absorption peak of the aromatic ring structure in the FTIR spectrum confirms the occurrence of a lignin degradation process. It was validated by an increase in the crystallinity index (CrI) of mesocarp fiber biomass subjected to a hybrid ozonation-ultrasonic pretreatment process and reinforced by changes in the surface structure of lignocellulosic biomass as shown in the results of SEM micrographs. Therefore, the results of this study can be used as a reference to increase the percentage of lignin degradation in lignocellulosic biomass.

ACKNOWLEDGEMENTS

This work is supported by a source of funds other than the APBN DIPA Universitas Diponegoro for the 2022 Fiscal Year. Number: 118-28/UN7.6.1/PP/2021

REFERENCES

[1] Megashah LN, Ariffin H, Zakaria MR, Hassan MA. (2018). Properties of Cellulose Extract from Different Types of Oil Palm Biomass. IOP Conference Series: Materials Science and Engineering, 368. https://doi.org/10.1088/1757-899X/368/1/012049

[2] Dirkes R, Neubauer PR, Rabenhorst J. (2021). Pressed Sap from Oil Palm (Elaeis guineensis) Trunks: a Revolutionary Growth Medium for the Biotechnological Industry. Biofuels, Bioproducts and Biorefining, 15, 931–44. https://doi.org/10.1002/bbb.2201

[3] OECD/FAO. (2018). OECD FAO Agricultural Outlook 2018 2027 Oilseeds and Oilseed Products. 127–38. https://doi.org/10.1787/agr_outlook-2018-7-en

[4] Hossain MA, Jewaratnam J, Ganesan P. (2016). Prospect of Hydrogen Production from Oil Palm Biomass by Thermochemical Process – A Review. International Journal of Hydrogen Energy, Elsevier Ltd. 41, 16637–55. https://doi.org/10.1016/j.ijhydene.2016.07.104

[5] Wan Omar WNN, Amin NAS. (2016). Multi Response Optimization of Oil Palm Frond Pretreatment By Ozonolysis. Industrial Crops and Products, Elsevier B.V. 85, 389–402. https://doi.org/10.1016/j.indcrop.2016.01.027

[6] Travaini R, Martín-Juárez J, Lorenzo-Hernando A, Bolado-Rodríguez S. (2016). Ozonolysis: An Advantageous Pretreatment for Lignocellulosic Biomass Revisited. Bioresource Technology, Elsevier Ltd. 199, 2–12. https://doi.org/10.1016/j.biortech.2015.08.143

[7] Kabir G, Mohd Din AT, Hameed BH. (2017). Pyrolysis of Oil Palm Mesocarp Fiber and Palm Frond in a Slow-Heating Fixed-Bed Reactor: A Comparative Study. Bioresource Technology, Elsevier Ltd. 241, 563–72. https://doi.org/10.1016/j.biortech.2017.05.180

[8] Okolie JA, Epelle EI, Tabat ME, Orivri U, Amenaghawon AN, Okoye PU. (2022). Waste Biomass Valorization for The Production of Biofuels and Value-Added Products: A Comprehensive Review of Thermochemical, Biological and Integrated Processes. Process Safety and Environmental Protection, Elsevier. 159, 323–44. https://doi.org/10.1016/j.psep.2021.12.049

[9] Lee KM, Quek JD, Tey WY, Lim S, Kang HS, Quen LK. (2022). Biomass Valorization by Integrating Ultrasonication and Deep Eutectic Solvents: Delignification, Cellulose Digestibility and Solvent Reuse. Biochemical Engineering Journal, Elsevier B.V. 187, 108587. https://doi.org/10.1016/j.bej.2022.108587

[10] Baksi S, Saha S, Birgen C, Sarkar U, Preisig HA, Markussen S. (2019). Valorization of Lignocellulosic Waste (Crotalaria juncea) Using Alkaline Peroxide Pretreatment under Different Process Conditions: An Optimization Study on Separation of Lignin, Cellulose, and Hemicellulose. Journal of Natural Fibers, Taylor & Francis. 16, 662–76. https://doi.org/10.1080/15440478.2018.1431998

[11] Chauhan R, Dinesh GK, Alawa B, Chakma S. (2021). A critical Analysis of Sono-Hybrid Advanced Oxidation Process of Ferrioxalate System for Degradation of Recalcitrant Pollutants. Chemosphere, Elsevier Ltd. 277, 130324. https://doi.org/10.1016/j.chemosphere.2021.130324

[12] Li S, Yang Y, Zheng H, Zheng Y, Jing T, Ma J. et al. (2022). Advanced Oxidation Process Based on Hydroxyl and Sulfate Radicals to Degrade Refractory Organic Pollutants in Landfill Leachate. Chemosphere, Elsevier Ltd. 297, 134214. https://doi.org/10.1016/j.chemosphere.2022.134214

[13] Heebner A, Abbassi B. (2022). Electrolysis Catalyzed Ozonation for Advanced Wastewater Treatment. Journal of Water Process Engineering, Elsevier Ltd. 46, 102638. https://doi.org/10.1016/j.jwpe.2022.102638

[14] Nagels M, Verhoeven B, Larché N, Dewil R, Rossi B. (2022). Corrosion Behaviour of Lean Duplex Stainless Steel in Advanced Oxidation Process (AOP) Based Wastewater Treatment Plants. Engineering Failure Analysis, 136. https://doi.org/10.1016/j.engfailanal.2022.106170

[15] Kiyanmehr K, Moussavi G, Mohammadi S, Naddafi K, Giannakis S. (2022). The Efficacy of The VUV/O3 Process Run in A Continuous-Flow Fluidized Bed Reactor for Simultaneous Elimination of Favipiravir and Bacteria in Aqueous Matrices. Chemosphere, Elsevier Ltd. 304, 135307. https://doi.org/10.1016/j.chemosphere.2022.135307

[16] Barrera-Martínez I, Guzmán N, Peña E, Vázquez T, Cerón-Camacho R, Folch J. et al. (2016). Ozonolysis of Alkaline Lignin and Sugarcane Bagasse: Structural Changes and Their Effect on Saccharification. Biomass and Bioenergy, 94, 167–72. https://doi.org/10.1016/j.biombioe.2016.08.010

[17] Suzuki H, Araki S, Yamamoto H. (2015). Evaluation of Advanced Oxidation Processes (AOP) Using O3, UV, and Tio2 for The Degradation of Phenol in Water. Journal of Water Process Engineering, Elsevier Ltd. 7, 54–60. https://doi.org/10.1016/j.jwpe.2015.04.011

[18] Praptyana IR, Budiyono. (2022). Biohydrogen Production from Wood Dust Mahogany (Swietenia Mahagony) By Dark Fermentation Using Enterobacter Aerogenes: Effect of Ozone Pretreatment Time and Ph. Materials Today: Proceedings, Elsevier Ltd. 63, S203–9. https://doi.org/10.1016/j.matpr.2022.02.406

[19] Hassaan MA, Nemr AEl, Elkatory MR, Eleryan A, Ragab S, Sikaily AEl et al. (2021). Enhancement of Biogas Production from Macroalgae Ulva Latuca Via Ozonation Pretreatment. Energies, 14, 1–16. https://doi.org/10.3390/en14061703

[20] Heidari Z, Pelalak R, Eshaghi MR, Pishnamazi M, Rezakazemi M, Aminabhavi TM. et al. (2022). A New Insight Into Catalytic Ozonation of Sulfasalazine Antibiotic by Plasma-Treated Limonite Nanostructures: Experimental, Modeling and Mechanism. Chemical Engineering Journal, Elsevier B.V. 428, 131230. https://doi.org/10.1016/j.cej.2021.131230

[21] Ngo Thi TD, Nguyen LH, Nguyen XH, Phung HV, The Vinh TH, Van Viet P et al. (2022). Enhanced Heterogeneous Photocatalytic Perozone Degradation of Amoxicillin by ZnO Modified TiO2 Nanocomposites under Visible Light Irradiation. Materials Science in Semiconductor Processing, Elsevier Ltd. 142, 106456. https://doi.org/10.1016/j.mssp.2022.106456

[22] Barik AJ, Gogate PR. (2018). Hybrid Treatment Strategies for 2,4,6-Trichlorophenol Degradation Based on Combination of Hydrodynamic Cavitation and AOPs. Ultrasonics Sonochemistry, Elsevier. 40, 383–94. https://doi.org/10.1016/j.ultsonch.2017.07.029

[23] Ran J, Duan H, Srinivasakannan C, Yao J, Yin S, Zhang L. (2022). Effective Removal of Organics from Bayer Liquor Through Combined Sonolysis and Ozonation: Kinetics and Mechanism. Ultrasonics Sonochemistry, Elsevier B.V. 88, 106106. https://doi.org/10.1016/j.ultsonch.2022.106106

[24] Fan X, Cao T, Yu X, Wang Y, Xiao X, Li F et al. (2020). The Evolutionary Behavior of Chromophoric Brown Carbon During Ozone Aging of Fine Particles from Biomass Burning. Atmospheric Chemistry and Physics, 20, 4593–605. https://doi.org/10.5194/acp-20-4593-2020

[25] Abdurahman MH, Abdullah AZ. (2020). Mechanism and Reaction Kinetic of Hybrid Ozonation-Ultrasonication Treatment for Intensified Degradation of Emerging Organic Contaminants in Water: A Critical Review. Chemical Engineering and Processing - Process Intensification, Elsevier. 154, 108047. https://doi.org/10.1016/j.cep.2020.108047

[26] Shen Y, Xu Q, Wei R, Ma J, Wang Y. (2017). Mechanism and Dynamic Study of Reactive Red X-3B Dye Degradation By Ultrasonic-Assisted Ozone Oxidation Process. Ultrasonics Sonochemistry, Elsevier B.V. 38, 681–92. https://doi.org/10.1016/j.ultsonch.2016.08.006

[27] Weavers LK, Hoffmann MR. (1998). Sonolytic Decomposition of Ozone in Aqueous Solution: Mass Transfer Effects. Environmental Science and Technology, 32, 3941–7. https://doi.org/10.1021/es980620o

[28] Candido RG, Gonçalves AR. (2019). Evaluation of Two Different Applications for Cellulose Isolated from Sugarcane Bagasse in a Biorefinery Concept. Industrial Crops and Products, 142. https://doi.org/10.1016/j.indcrop.2019.111616

[29] Montgomery. (1991). Debris Flow Hazard Mitigation for Colluvium-Filled Swales.

[30] Dagnino EP, Felissia FE, Chamorro E, Area MC. (2017). Optimization of The Soda-Ethanol Delignification Stage for a Rice Husk Biorefinery. Industrial Crops and Products, Elsevier B.V. 97, 156–65. https://doi.org/10.1016/j.indcrop.2016.12.016

[31] Wu Y, Yao S, Narale BA, Shanmugam A, Mettu S, Ashokkumar M. (2022). Ultrasonic Processing of Food Waste to Generate Value-Added Products. Foods, 11. https://doi.org/10.3390/foods11142035

[32] Segal L, Creely JJ, Martin AE, Conrad CM. (1959). An Empirical Method for Estimating the Degree of Crystallinity of Native Cellulose Using the X-Ray Diffractometer. Textile Research Journal, 29, 786–94. https://doi.org/10.1177/004051755902901003

[33] Vanholme R, Morreel K, Ralph J, Boerjan W. (2008). Lignin Engineering. Current Opinion in Plant Biology, 11, 278–85. https://doi.org/10.1016/j.pbi.2008.03.005

[34] Anuar TATY, Ariffin H, Norrrahim MNF, Hassan MA. (2017). Factors Affecting Spinnability of Oil Palm Mesocarp Fiber Cellulose Solution for The Production of Microfiber. BioResources, 12, 715–34. https://doi.org/10.15376/biores.12.1.715-734

[35] Megashah LN, Ariffin H, Zakaria MR, Ando Y. (2018). Characteristics of Cellulose from Oil Palm Mesocarp Fibres Extracted by Multi-Step Pretreatment Methods. IOP Conference Series: Materials Science and Engineering, 368. https://doi.org/10.1088/1757-899X/368/1/012001

[36] Rizal NFAA, Ibrahim MF, Zakaria MR, Bahrin EK, Abd-Aziz S, Hassan MA. (2018). Combination of Superheated Steam with Laccase Pretreatment Together with Size Reduction to Enhance Enzymatic Hydrolysis of Oil Palm Biomass. Molecules, 23. https://doi.org/10.3390/molecules23040811

[37] Azlan N, Mohd, Lin C, Gan S, Basyaruddin M, Rahman A. (2022). Materials Today : Proceedings Effectiveness of Various Solvents In The Microwave-Assisted Extraction of Cellulose from Oil Palm Mesocarp Fiber. Materials Today: Proceedings, Elsevier Ltd. https://doi.org/10.1016/j.matpr.2021.12.086

[38] Olughu, Onu Onu, Tabil, Lope G, Dumonceaux, Dan, T. (2021). Ultrasonic Delignification and Microstructural Characterization of Switchgrass (In Indonesia).

[39] Mukherjee A, Banerjee S, Halder G. (2018). Parametric Optimization of Delignification of Rice Straw Through Central Composite Design Approach Towards Application in Grafting. Journal of Advanced Research, Cairo University. 14, 11–23. https://doi.org/10.1016/j.jare.2018.05.004

[40] Prasetyaningrum A, Ratnawati R, Jos B. (2017). Optimization of the Ozonation Process on Depolymerization of κ-Carrageenan with the Response Surface Method (In Indonesia). Reaktor, 17, 1. https://doi.org/10.14710/reaktor.17.1.1-8

[41] Mostapha M, Azamkamal F, Mohd Salleh K, Amran UA, Gan S, Zakaria S. (2021). Parameter Optimization for Esterified Palm Oil Empty Fruit Bunches (EFB) Cellulose (In Indonesia). Sains Malaysiana, 50, 3719–32. https://doi.org/10.17576/jsm-2021-5012-21

[42] Ramadoss G, Muthukumar K. (2016). Mechanistic Study on Ultrasound Assisted Pretreatment of Sugarcane Bagasse Using Metal Salt With Hydrogen Peroxide for Bioethanol Production. Ultrasonics Sonochemistry, 28, 207–17. https://doi.org/10.1016/j.ultsonch.2015.07.006

[43] Pujokaroni AS, Ohtani Y, Ichiura H. (2020). Ozone Treatment for Improving The Solubility of Cellulose Extracted from Palm Fiber. Journal of Applied Polymer Science, 138, 1–11. https://doi.org/10.1002/app.49610

[44] Cubero MTG, Palacín LG, González-Benito G, Bolado S, Lucas S, Coca M. (2012). An Analysis of Lignin Removal in A Fixed Bed Reactor By Reaction of Cereal Straws With Ozone. Bioresource Technology, 107, 229–34. https://doi.org/10.1016/j.biortech.2011.12.010

[45] Ruan XC, Liu MY, Zeng QF, Ding YH. (2010). Degradation and Decolorization of Reactive Red X-3B Aqueous Solution By Ozone Integrated with Internal Micro-Electrolysisa. Separation and Purification Technology, Elsevier B.V. 74, 195–201. https://doi.org/10.1016/j.seppur.2010.06.005

[46] Chiha M, Hamdaoui O, Baup S, Gondrexon N. (2011). Sonolytic Degradation of Endocrine Disrupting Chemical 4-Cumylphenol in Water. Ultrasonics Sonochemistry, Elsevier B.V. 18, 943–50. https://doi.org/10.1016/j.ultsonch.2010.12.014

[47] Gągol M, Przyjazny A, Boczkaj G. (2018). Effective Method of Treatment of Industrial Effluents under Basic pH Conditions using Acoustic Cavitation – A Comprehensive Comparison with Hydrodynamic Cavitation Processes. Chemical Engineering and Processing - Process Intensification, 128, 103–13. https://doi.org/10.1016/j.cep.2018.04.010

[48] Wang T, Le T, Hu J, Ravindra AV, Xv H, Zhang L et al. (2022). Ultrasonic-Assisted Ozone Degradation of Organic Pollutants in Industrial Sulfuric Acid. Ultrasonics Sonochemistry, Elsevier B.V. 86, 106043. https://doi.org/10.1016/j.ultsonch.2022.106043

[49] Xiong X, Wang B, Zhu W, Tian K, Zhang H. (2019). A Review on Ultrasonic Catalytic Microbubbles Ozonation Processes: Properties, Hydroxyl Radicals Generation Pathway and Potential in Application. Catalysts, 9. https://doi.org/10.3390/catal9010010

[50] Zhao L, Ma W, Ma J, Wen G, Liu Q. (2015). Relationship Between Acceleration of Hydroxyl Radical Initiation and Increase of Multiple-Ultrasonic Field Amount in the Process of Ultrasound Catalytic Ozonation for Degradation of Nitrobenzene in Aqueous Solution. Ultrasonics Sonochemistry, Elsevier B.V. 22, 198–204. https://doi.org/10.1016/j.ultsonch.2014.07.014

[51] Arantes V, Jellison J, Goodell B. (2012). Peculiarities of Brown-rot Fungi and Biochemical Fenton Reaction with Regard to Their Potential as a Model for Bioprocessing Biomass. Applied Microbiology and Biotechnology, 94, 323–38. https://doi.org/10.1007/s00253-012-3954-y

[52] Maqsood HS, Bashir U, Wiener J, Puchalski M, Sztajnowski S, Militky J. (2017). Ozone Treatment of Jute Fibers. Cellulose, Springer Netherlands. 24, 1543–53. https://doi.org/10.1007/s10570-016-1164-y

[53] Martínez AT, Rencoret J, Nieto L, Jiménez-Barbero J, Gutiérrez A, Del Río JC. (2011). Selective Lignin and Polysaccharide Removal in Natural Fungal Decay of Wood as Evidenced by in Situ Structural Analyses. Environmental Microbiology, 13, 96–107. https://doi.org/10.1111/j.1462-2920.2010.02312.x

[54] Chieng BW, Lee SH, Ibrahim NA, Then YY, Loo YY. (2017). Isolation And Characterization Of Cellulose Nanocrystals From Oil Palm Mesocarp Fiber. Polymers, 9, 1–11. https://doi.org/10.3390/polym9080355

[55] Okahisa Y, Furukawa Y, Ishimoto K, Narita C, Intharapichai K, Ohara H. (2018). Comparison of Cellulose Nanofiber Properties Produced from Different Parts of The Oil Palm Tree. Carbohydrate Polymers, 198, 313–9. https://doi.org/10.1016/j.carbpol.2018.06.089

[56] Rosli NA, Ahmad I, Abdullah I. (2013). Isolation and Characterization of Cellulose Nanocrystals from Agave Angustifolia Fibre. BioResources, 8, 1893–908. https://doi.org/10.15376/biores.8.2.1893-1908

[57] Bogolitsyn K, Parshina A, Aleshina L. (2020). Structural Features of Brown Algae Cellulose. Cellulose, Springer Netherlands. 27, 9787–800. https://doi.org/10.1007/s10570-020-03485-z

[58] Gonzalez M, Pereira-Rojas J, Villanueva I, Agüero B, Silva I, Velasquez I et al. (2022). Preparation and Characterization of Cellulose Fibers from Meghatyrsus Maximus: Applications in its Chemical Derivatives. Carbohydrate Polymers, Elsevier Ltd. 296, 119918. https://doi.org/10.1016/j.carbpol.2022.119918

[59] Reddy KO, Maheswari CU, Dhlamini MS, Mothudi BM, Kommula VP, Zhang J et al. (2018). Extraction and Characterization of Cellulose Single Fibers from Native African Napier Grass. Carbohydrate Polymers, Elsevier Ltd. 188, 85–91. https://doi.org/10.1016/j.carbpol.2018.01.110

[60] Zhang K, Si M, Liu D, Zhuo S, Liu M, Liu H, et al. (2018). A Bionic System with Fenton Reaction and Bacteria as A Model for Bioprocessing Lignocellulosic Biomass. Biotechnology for Biofuels, BioMed Central. 11, 1–14. https://doi.org/10.1186/s13068-018-1035-x

[61] Valladares-Diestra KK, Porto de Souza Vandenberghe L, Zevallos Torres LA, Nishida VS, Zandoná Filho A, Woiciechowski AL, et al. (2021). Imidazole Green Solvent Pre-Treatment as A Strategy for Second-Generation Bioethanol Production from Sugarcane Bagasse. Chemical Engineering Journal, 420. https://doi.org/10.1016/j.cej.2020.127708

[62] Rasid NSA, Zainol MM, Amin NAS. (2021). Synthesis and Characterization of Carboxymethyl Cellulose Derived from Empty Fruit Bunch. Sains Malaysiana, 50, 2523–35. https://doi.org/10.17576/jsm-2021-5009-03

[63] Zulnazri Adha, muhammad ikhwanul, Dewi R. (2022). Experimental Study of Cellulose Extraction from Oil Palm Empty Fruits Bunches. 7–14. https://doi.org/10.31284/j.iptek.2022.v26i1.2

[64] Lu H, Liu S, Shi Y, Chen Q. (2022). Efficient Delignification of Sugarcane Bagasse by Fenton Oxidation Coupled with Ultrasound-Assisted NaOH for Biotransformation from Agaricus Sinodeliciosus Var. Chaidam. Chemical Engineering Journal, Elsevier B.V. 448, 137719. https://doi.org/10.1016/j.cej.2022.137719

[65] Ren X, Zhang X, Liang Q, Hou T, Zhou H. (2017). Effects of Different Working Modes of Ultrasound on Structural Characteristics of Zein and ACE Inhibitory Activity of Hydrolysates. Journal of Food Quality, 2017. https://doi.org/10.1155/2017/7896037